The functional proteome landscape of *Escherichia coli*

André Mateus[1], Johannes Hevler[1], Jacob Bobonis[1,2], Nils Kurzawa[1,2], Malay Shah[1], Karin Mitosch[1], Camille V. Goemans[1], Dominic Helm[3], Frank Stein[3], Athanasios Typas[1,*], Mikhail M. Savitski[1,*]

[1]European Molecular Biology Laboratory, Genome Biology Unit, Meyerhofstr. 1, 69117 Heidelberg, Germany.

[2]Candidate for joint PhD degree from EMBL and Heidelberg University, Faculty of Biosciences, 69120 Heidelberg, Germany

[3]European Molecular Biology Laboratory, Proteomics core facility, Meyerhofstr. 1, 69117 Heidelberg, Germany.

*Corresponding authors:

Mikhail M. Savitski

Email: mikhail.savitski@embl.de

Athanasios Typas

Email: athanasios.typas@embl.de

Phone: +49 6221 387-8560

Contents

Supplementary Figures

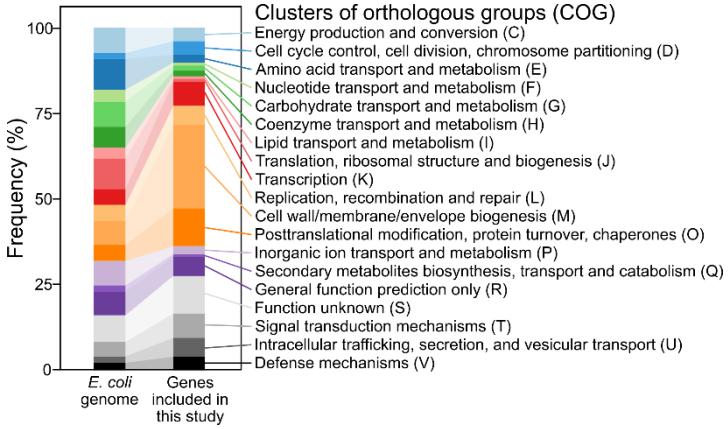

Supplementary Figure 1. Cellular processes targeted in this study. Distribution of cellular processes targeted in this study compared to the general distribution of the *E. coli* genome using Clusters of Orthologous Groups (COG)[1].

Supplementary Figure 2. Layout of mass spectrometry runs. Mutants in each MS run are selected in a way that minimized the correlation of chemical genetic fingerprints[2] of each mutant with those present in the same row or column—to ensure that they targeted different processes (see Online methods for details). The 22 MS runs in this study are represented as columns (biological replicate 1) or rows (biological replicate 2). Distribution of Pearson correlation coefficient of growth phenotypes of the mutant with all the other mutants included in the two replicate MS runs—based on the data from Herrera-Dominguez et al.[2]. Box plots are depicted as in **Figure 2a** (n=20 for all box plots).

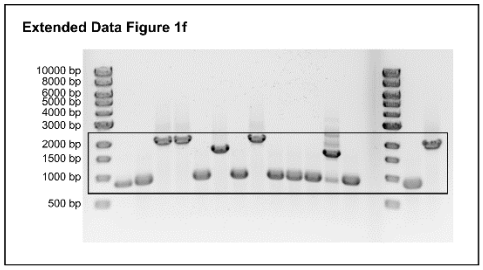

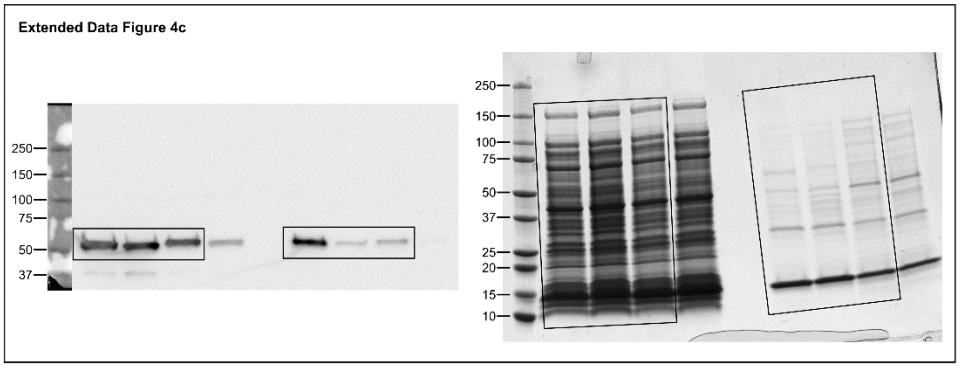

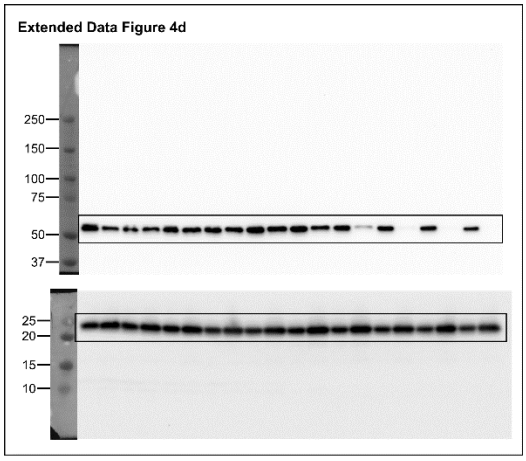

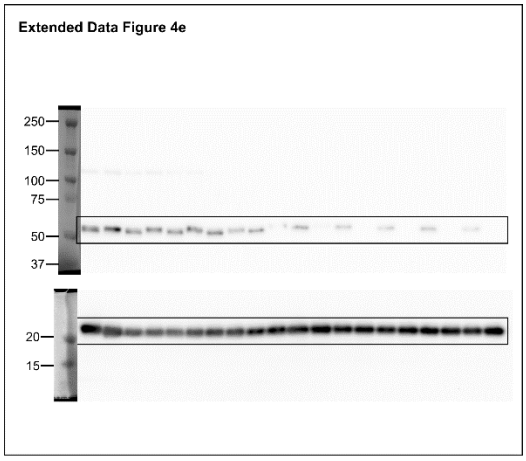

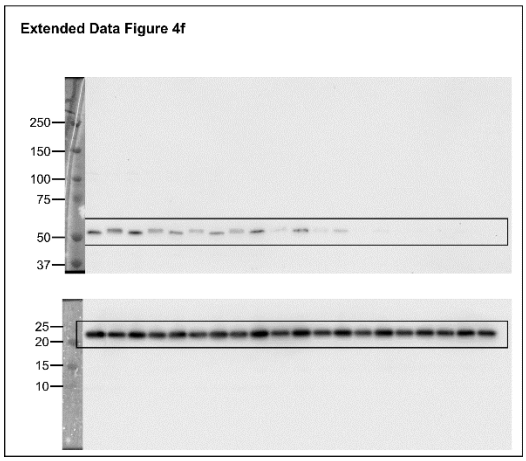

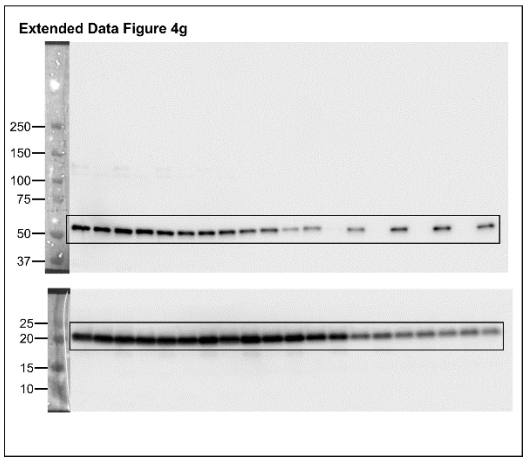

Supplementary Figure 3. Uncropped gels and blots for Extended Data Figure 1f and Extended Data Figure 4c-g.

Supplementary Discussion

Differences in biological replicates are attributable to biological phenomena

Measurements were largely consistent across biological replicates (95% of the replicate values of $\log_2$ fold-change compared to control (all proteins, all temperatures, all mutants) were within 1.7-fold of each other; **Extended Data Figure 1b**), despite showing only a moderate correlation (Pearson correlation coefficient (r)=0.50; **Extended Data Figure 1c**) that was independent of the temperature measured (**Extended Data Figure 1d**). The correlation was higher (r=0.77) for mutants for which we had only one clone available and probed it twice in biological replicates (n=7; **Supplementary Data 1**). This suggested that for some mutants in the Keio collection, the two constructed clones have genetic differences, something that is not uncommon in systematic mutant libraries[3-5]. Therefore, we analyzed proteins which were consistently variable across replicates, and found that these were enriched in motility- and chemotaxis-related proteins (e.g., multiple flagellar proteins, CheY, CheW, Tar, and Tsr), among other specific processes (**Supplementary Data 4**). Variable proteins were consistently co-regulated within each replicate of our experiments, being either all up- or downregulated in one of the two clones (**Extended Data Figure 1e**). Motility genes were recently shown to be upregulated in a large proportion of the Keio library strains, due to the presence of insertion sequence elements upstream of the promoter of the flagellar master regulator (FlhDC), which restored its expression[3]. Therefore, we selected seven mutants in which one of the clones showed high expression of motility-related proteins, and confirmed that for six of them, the clone with high expression did indeed contain insertion elements upstream of the *flhDC* operon (Δ*fur* presumably has different point-mutations reactivating *flhDC* expression[3]; **Extended Data Figure 1f**). Thus, the differences between clone behavior are likely due to true biological phenomena, and in the case of motility, due to secondary mutations.

Changes in protein thermal stability reflect protein function

We assessed the impact that each *E. coli* mutant elicited in the proteome. On average, each mutant affected 27 proteins in abundance (range: 0-159) and 41 proteins in thermal stability (range: 1-117) (**Extended Data Figure 1i**). Some genetic perturbations led to a large number of significant proteome changes, such as those targeting the essential genes *bamA* (255 proteins altered in abundance or thermal stability), *ftsA* (225 proteins), or *lptD* (94 proteins), while others led to only a few changes, such as those targeting genes of unknown function, e.g., Δ*yieP* (18 proteins), Δ*yfeD* (20 proteins), or Δ*ypjD* (20 proteins). There was a general trend for mutants with more changes in abundance to also have more changes in thermal stability (r_S=0.70), yet some genetic perturbations led almost exclusively to changes in thermal stability. For example, Δ*mrcB* (80 proteins changing in thermal stability, no changes in protein abundance) and Δ*lpoB* (74 proteins changing in thermal stability and 6 in abundance)—MrcB and LpoB form a complex involved in cell wall biosynthesis[6]. These changes are driven by multiple mechanisms, from protein interactions with other proteins, metabolites or nucleic acids, to changes to the protein environment or post-translational modifications, as we elaborate with examples below.

As previously observed[7], deletion of protein complex members generally led to the thermal destabilization of other members of the complex. An exception was the outer membrane components of the ExbBD-TonB components that were generally thermally stabilized (**Extended Data Figure 2a**). Interestingly, not all protein complex members were thermally destabilized upon the deletion of one of the members. For example, both AcrA and AcrB were thermally destabilized in Δ*tolC*, while only AcrB was thermally

destabilized in Δ*acrA* and AcrA in Δ*acrB*; only SdhB was thermally destabilized in Δ*sdhA*; only NuoG was thermally destabilized in Δ*nuoF*. The abundance of these subunits was not directly linked to their thermal stability (**Extended Data Figure 2b**), since some deletions led to the upregulation of the other complex members (e.g., AcrA and AcrB in Δ*tolC*; or SdhB in Δ*sdhA*), others led to their downregulation (e.g., AcrB in Δ*acrA*), while some led to no changes (e.g., all other subunits of the respiratory complex I in Δ*nuoF*). These results suggest that although other complex members and direct interactions generally help a protein to acquire more robust folds (and hence be more thermally stable), some complex members (TolC) or sub-complexes (Fo ATP synthase complex) fold and exist independently of the other parts of the complex. Further, the cell seems to sense and react differently to the faulty assembly of certain complexes, by either upregulating the expression other complex members in an attempt to compensate (Δ*tolC*), or by downregulating expression or promoting degradation of improperly assembled complexes (ATP synthase).

We also observed that more general alterations in cell physiology led to changes in protein thermal stability. An example of this are the changes in outer membrane composition caused by defects in lipopolysaccharide biosynthesis in Δ*rfaC* (Δ*waaC*), Δ*rfaF* (Δ*waaF*) and Δ*lapA* mutants, which led to thermal stability changes in multiple outer membrane proteins. In these three mutants, >30% of the thermal stability hits were outer membrane proteins (compared to an average of 4% of detected proteins being located in the outer membrane[8]; $p < 10^{-17}$ for the three mutants in a Fisher's exact test). This is likely caused by the different LPS content and environment in the outer membrane[9].

A large number of proteins known to bind cofactors were also affected. For example, we observed a general thermal destabilization of iron-sulfur cluster binding proteins (based on gene ontology annotations) in the iron-sulfur cluster biosynthesis mutants, Δ*iscA*, Δ*iscS*, and Δ*iscU* (**Extended Data Figure 4a**). We observed multiple proteins that were thermally destabilized in the three mutants, but not annotated as iron-sulfur cluster binding proteins. These included Edd, FrdA, GltD, NsrR, NuoC, SdaA, SdhA, YdbK, which are all known or predicted to bind iron-sulfur clusters. In the molybdopterin biosynthesis mutant, Δ*moaE*, we observed a thermal destabilization of FdoG (thermal stability z-score=-13.9) and FdoH (thermal stability z-score=-10.4)—two molybdopterin binding proteins[10]. The orphan proteins YcbX (thermal stability z-score=-7.5) and YiiM (thermal stability z-score=-5.1) were also thermally destabilized in Δ*moaE*, in agreement with the prediction that they bind molybdopterin[11]. We also observed the thermal destabilization of the periplasmic copper oxidase CueO in the Δ*tatB* mutant (thermal stability z-score=-12.7; **Extended Data Figure 4b**). CueO is translocated from the cytosol to the periplasm by the Tat system[12]. The Tat system recognizes an N-terminal signal peptide in CueO, which is cleaved upon translocation. To assess the reason for CueO thermal destabilization, we deleted its signal peptide (Δ28-CueO), fused it to a FLAG peptide at the C-terminus, and expressed it from a plasmid in a Δ*cueO* strain. As expected, this construct abolished translocation of CueO, bringing periplasmic CueO to basal levels, similar to that of full length CueO in a Δ*tatB* strain (**Extended Data Figure 4c**). Phenocopying the full length CueO in Δ*tatB* (**Extended Data Figure 4e**), the Δ28-CueO was thermally destabilized even in the presence of TatB (**Extended Data Figure 4d and f**). This confirms previous findings that only the periplasmic fraction of CueO can bind copper[13,14], and strongly suggests that the higher thermal stability of the periplasmic CueO is due to copper binding. Yet, it is not the periplasmic location *per se* that selectively switches CueO to an active form that can bind copper. It is rather the lack of copper in the cytoplasm which prevents CueO from being thermally stabilized in the cytoplasm, as the Δ28-CueO could be thermally stabilized in lysate when copper chloride was added (**Extended Data Figure 4g**).

In general, it is possible to rationalize many of the cellular changes as a direct consequence of the genetic perturbation—exemplified in this work by changes in ligand levels (metabolite, protein or cofactor) and protein environment. Previously, we have observed that nucleic acid binding[15] and post-translational modifications[16-18] can also lead to changes in protein thermal stability, and are likely to explain further proteome alterations observed here. However, many changes may be due to more complex and indirect cellular responses. Both direct and indirect links contribute alike to our ability to capture new functional interactions in a guilt-by-association manner.

Protein co-expression and co-melting capture different functional associations

To identify drivers of strong correlation for functionally-associated proteins, we calculated the Spearman's rank correlation between protein pairs based on their abundance or thermal stability changes alone. Despite being less powerful (only a maximum of 121 data points were used to calculate these correlations) than correlations based to all $\log_2$ fold-changes (up to 1210 points per protein), proteins that belonged to the same operon had stronger correlations in their abundance levels than in their thermal stability (**Extended Data Figure 6c**). This was similar for protein pairs that belong to the same complex, particularly because a large fraction (38%) of these are also part of the same operon (**Extended Data Figure 6d**). In this case, protein thermal stability allows finding within complex interactions (see 'Protein co-expression and co-melting capture different functional associations'). For metabolic pathways, this was dependent on the protein pair, with some showing strong correlations in their thermal stability, but not abundance levels (**Extended Data Figure 6e**). A case-in-point are the enzymes of UDP-N-acetylmuramoyl-pentapeptide biosynthesis pathway, a precursor of peptidoglycan (**Extended Data Figure 6f**), for which there was a strong correlation between the thermal stability of DdlA and MurC (r_S=0.79; **Extended Data Figure 6g**) or DdlA and MurF (r_S=0.73), while abundance levels were not linked (r_S (DdlA-MurC)=-0.13 and r_S (DdlA-MurF)=-0.06). DdlA thermal stability was also moderately correlated with the thermal stability of MurA (r_S=0.51) and MurB (r_S=0.49). MurC, MurD, MurE, MurF, MurG, and MraY (all encoded in the same operon) showed a stronger correlation in their abundance levels (**Extended Data Figure 6h**).

In summary, this approach offers another way to look at the data that could expand the annotation of functionally-associated protein pairs, particularly in cases in which both abundance and thermal stability are altered, but only one of them is coordinated. These data are available to be explored at http://ecoliTPP.shiny.embl.de.

Protein co-expression and co-melting patterns capture regulatory relationships and protein complex architecture

Apart from the general correlation, as summarized by the Spearman's rank correlation, a closer look at how some protein pairs behave can reveal interesting aspects of protein regulation. For example, the outer membrane porin OmpF and the periplasmic protease DegP showed one of the strongest anti-correlations (r_S=-0.58; **Extended Data Figure 3a**). This anti-correlation was driven by changes in protein expression, generally with OmpF being downregulated and DegP being upregulated. The levels of these two proteins are known to be regulated by the Cpx signal transduction system upon cell envelope stress (**Extended Data Figure 3b**)[19]. In accordance, the mutants responsible for the changes in abundance of these proteins are known to cause envelope stress (e.g., Δ*rfaC*, Δ*rfaF*, Δ*surA*, and Δ*cpxA*). Interestingly, Δ*ompR* was an

outlier in this correlation, in that it only affected levels of OmpF. This is in agreement with OmpR affecting only *ompF* transcription (**Extended Data Figure 3b**)[20].

Functionally-associated proteins, such as those belonging to the same complexes, were generally highly correlated across genetic perturbations. However, a closer look at specific complexes showed substructure in these. For example, the ribosome contained three large clusters (two of them could be split further into subclusters; **Extended Data Figure 7a**), separating the components of the 30S and the 50S subunits in a rather accurate manner (**Extended Data Figure 7a and c**). The smallest of these clusters (left most cluster in **Extended Data Figure 7a**) included proteins with weak correlations to most other ribosomal proteins (RpsU, RplL, RpmC, RplJ, and RpsA). These proteins are structurally distinct subunits of the ribosome, e.g., RpsU belongs to the 30S subunit, but is also known to associate with the 50S subunit[21]; RplJ and RplL belong to the ribosomal lateral stalk[22]; and RpsA is known to not always be associated with the ribosome[23]. Coloring the subunits of a high-resolution structure of the ribosome[24] (PDB: 4YBB) revealed that members of the same cluster are commonly physically close to each other (**Extended Data Figure 7a-b**). Similar substructures could be observed for the ATP synthase (PDB: 5T4O; **Extended Data Figure 7d-e**) and the respiratory complex I (PDB: 4HEA; **Extended Data Figure 7f-g**). We further calculated the distance between the centers-of-mass of all subunit pairs of each of these complexes as a proxy for distance (**Extended Data Figure 7a, d, and e**), and observed that strongly correlating subunits were generally at a shorter distance from each other ($r=-0.21$, $p<10^{-11}$; **Extended Data Figure 7h**). Therefore, these proteins are likely to physically interact and melt coherently, as previously observed[7,15,25]. Indeed, although there was no correlation between strongly correlating subunits and their distance in the complex when considering only co-changes in protein abundance ($r_S=-0.025$, $p=0.4$), there was one when considering only thermal stability co-changes ($r_S=-0.25$, $p<10^{-16}$). Thus, it is the power of combining abundance and thermal stability that enables us to functionally annotate protein complexes (based on their abundance co-changes) and assess their physical interactions (based on their thermal stability co-changes). Using these data to characterize other protein complexes, might aid future structural biology studies.

GO enrichments of co-changing partners of proteins of unknown function can reveal their function

The gene ontology (GO) enrichment of the highly correlated proteins of each protein provided possible hints for the function of orphan proteins, with many of them being supported by previous studies (**Extended Data Figure 8**). For example, YcjX is part of the σ^{32} response which is related to heat stress[26]; YbiX is upregulated during iron suppression and YncE is hypothesized to be involved in iron acquisition[27]; YggX is reported to play a role in resistance to oxidation of iron-sulfur clusters[28]; WbbJ and WbbK are encoded in the same operon as other proteins involved in lipopolysaccharide biosynthesis; YbhC is an outer membrane lipoprotein[29], while YeaY has been predicted to be one based on its sequence[30]; YiaD is reported to be involved in the function of BamB, which is a member of the β-barrel assembly machinery[31]; the knockout mutants of YciI and YdiJ display a phenotypical fingerprint similar to other mutants of amino acid biosynthesis[2]; YagU expression is induced upon low pH stress[32] and we find a correlation between its thermal stability and survival at pH 4 ($r=0.38$, $p=0.009$)—this correlation was mostly driven by the thermal destabilization of YagU in Δ*cpxA*, in which other proteins involved in pH regulation are also downregulated (e.g., YdiY, DtpA, and NhaB), suggesting a possible mechanism for the sensitivity of Δ*cpxA* to acidic conditions; YaaA is important to protect against hydrogen peroxide treatment, which causes DNA damage[33]; YebC and YhgF are important for survival after ionizing radiation exposure[34]; YejK affects DNA

replication[35]; YcbZ has genetic interactions with multiple genes involved in translation and ribosome biogenesis[36].

Disentangling molecular mechanisms of protein interactions

While it is impossible to directly pinpoint the exact molecular function of an orphan protein or the molecular reason for why two proteins are functionally linked, the data presented here provide strong leads for further studies. First, it directly provides the means to infer the function in a guilt-by-association manner—i.e., if a protein is highly correlated with proteins from a certain biological process, it is likely that the protein is involved in that process. Second, it is possible to evaluate the reason two proteins are linked: if the correlation is driven by changes in protein abundance, it likely indicates co-regulation, while if they are driven by changes in thermal stability, it likely indicates a physical interaction (direct or mediated by a metabolite). Finally, it is possible to know which conditions drive the correlation. This might give direct insight into the interaction (e.g., by looking for mechanism of the perturbations, which can be further aided by evaluating which other proteins are affected in those mutants), or allow further studies in those perturbations (which might exacerbate the interaction and facilitate its observation).

Mutant phenotypes are explained by proteome changes beyond the deleted gene

We observed a moderate correlation between MdtK abundance and sensitivity to metformin[2] ($r=0.44$, $p<0.001$; **Extended Data Figure 10b**). MdtK is a multidrug efflux pump, which when deleted causes a severe fitness defect in the presence of metformin (S-score=-22.3)[2], and when overexpressed causes resistance to metformin[37]. Therefore, it likely reduces intracellular concentrations of metformin. We thus wondered if mutants with low MdtK abundance (Δ*ahpC* (abundance z-score=-4.4) and Δ*cpxA* (abundance z-score=-3.3)) were sensitive to metformin ($S\text{-score}_{\Delta ahpC}=-10.5$ and $S\text{-score}_{\Delta cpxA}=-6.5$) due to the low levels of this pump. To test this, we used plasmids to ectopically express *mdtK*, *ahpC* or *cpxA*, which in all cases complemented the corresponding mutant phenotype and restored the resistance to metformin (**Extended Data Figure 10c-d**). However, only *mdtK* ectopic expression could restore sensitivity of the non-cognate mutants (Δ*ahpC* and Δ*cpxA*) or that of the double mutants (Δ*mdtK*Δ*ahpC* and Δ*mdtK*Δ*cpxA*), demonstrating that MdtK levels are important for metformin sensitivity in these mutants.

We further noticed a correlation between RecR abundance and sensitivity to UV[38] ($r=0.53$, $p<10^{-4}$; **Extended Data Figure 10e**). RecR is a DNA repair protein and when absent, cells are sensitive to UV[38]. This correlation was mostly driven by the low levels of RecR in Δ*ybaB* (abundance z-score=-5.6), a gene located just upstream and in the same operon as *recR* (**Extended Data Figure 10f**). Therefore, we postulated that the UV sensitivity of Δ*ybaB* was due to the low abundance of RecR and not due to the lack of YbaB itself, as it has previously been suggested[39]. Indeed, only overexpression of *recR* (and not *ybaB*) in both Δ*ybaB* and Δ*recR* was able to recover UV sensitivity to the same level as wildtype cells (**Extended Data Figure 10g**), confirming our hypothesis.

References

1 Tatusov, R. L., Galperin, M. Y., Natale, D. A. & Koonin, E. V. The COG database: a tool for genome-scale analysis of protein functions and evolution. *Nucleic Acids Res* **28**, 33-36, doi:10.1093/nar/28.1.33 (2000).

2 Herrera-Dominguez, L. & Typas, A. https://ecoli-darkgen.shinyapps.io/app-1/. (2020).

3 Parker, D. J., Demetci, P. & Li, G. W. Rapid Accumulation of Motility-Activating Mutations in Resting Liquid Culture of Escherichia coli. *J Bacteriol* **201**, doi:10.1128/JB.00259-19 (2019).

4 Teng, X. *et al.* Genome-wide consequences of deleting any single gene. *Mol Cell* **52**, 485-494, doi:10.1016/j.molcel.2013.09.026 (2013).

5 Puddu, F. *et al.* Genome architecture and stability in the Saccharomyces cerevisiae knockout collection. *Nature* **573**, 416-420, doi:10.1038/s41586-019-1549-9 (2019).

6 Typas, A. *et al.* Regulation of peptidoglycan synthesis by outer-membrane proteins. *Cell* **143**, 1097-1109, doi:10.1016/j.cell.2010.11.038 (2010).

7 Mateus, A. *et al.* Thermal proteome profiling in bacteria: probing protein state in vivo. *Mol Syst Biol* **14**, e8242, doi:10.15252/msb.20188242 (2018).

8 Orfanoudaki, G. & Economou, A. Proteome-wide subcellular topologies of E. coli polypeptides database (STEPdb). *Mol Cell Proteomics* **13**, 3674-3687, doi:10.1074/mcp.O114.041137 (2014).

9 Brabetz, W., Muller-Loennies, S., Holst, O. & Brade, H. Deletion of the heptosyltransferase genes rfaC and rfaF in Escherichia coli K-12 results in an Re-type lipopolysaccharide with a high degree of 2-aminoethanol phosphate substitution. *Eur J Biochem* **247**, 716-724, doi:10.1111/j.1432-1033.1997.00716.x (1997).

10 Iobbi-Nivol, C. & Leimkuhler, S. Molybdenum enzymes, their maturation and molybdenum cofactor biosynthesis in Escherichia coli. *Biochim Biophys Acta* **1827**, 1086-1101, doi:10.1016/j.bbabio.2012.11.007 (2013).

11 Kozmin, S. G., Leroy, P., Pavlov, Y. I. & Schaaper, R. M. YcbX and yiiM, two novel determinants for resistance of Escherichia coli to N-hydroxylated base analogues. *Mol Microbiol* **68**, 51-65, doi:10.1111/j.1365-2958.2008.06128.x (2008).

12 Palmer, T. & Berks, B. C. The twin-arginine translocation (Tat) protein export pathway. *Nat Rev Microbiol* **10**, 483-496, doi:10.1038/nrmicro2814 (2012).

13 Stolle, P., Hou, B. & Bruser, T. The Tat Substrate CueO Is Transported in an Incomplete Folding State. *J Biol Chem* **291**, 13520-13528, doi:10.1074/jbc.M116.729103 (2016).

14 Grass, G. & Rensing, C. CueO is a multi-copper oxidase that confers copper tolerance in Escherichia coli. *Biochem Biophys Res Commun* **286**, 902-908, doi:10.1006/bbrc.2001.5474 (2001).

15 Becher, I. *et al.* Pervasive Protein Thermal Stability Variation during the Cell Cycle. *Cell* **173**, 1495-1507 e1418, doi:10.1016/j.cell.2018.03.053 (2018).

16 Huang, J. X. *et al.* High throughput discovery of functional protein modifications by Hotspot Thermal Profiling. *Nature Methods*, doi:10.1038/s41592-019-0499-3 (2019).

17 Potel, C. M. *et al.* Impact of phosphorylation on thermal stability of proteins. *bioRxiv*, 2020.2001.2014.903849, doi:10.1101/2020.01.14.903849 (2020).

18 Smith, I. R. *et al.* Identification of phosphosites that alter protein thermal stability. *bioRxiv*, 2020.2001.2014.904300, doi:10.1101/2020.01.14.904300 (2020).

19 Batchelor, E., Walthers, D., Kenney, L. J. & Goulian, M. The Escherichia coli CpxA-CpxR envelope stress response system regulates expression of the porins ompF and ompC. *J Bacteriol* **187**, 5723-5731, doi:10.1128/JB.187.16.5723-5731.2005 (2005).

20 Yoshida, T., Qin, L., Egger, L. A. & Inouye, M. Transcription regulation of ompF and ompC by a single transcription factor, OmpR. *J Biol Chem* **281**, 17114-17123, doi:10.1074/jbc.M602112200 (2006).

21 Odom, O. W., Deng, H. Y., Dabbs, E. R. & Hardesty, B. Binding of S21 to the 50S subunit and the effect of the 50S subunit on nonradiative energy transfer between the 3' end of 16S RNA and S21. *Biochemistry* **23**, 5069-5076, doi:10.1021/bi00316a037 (1984).
22 Choi, A. K., Wong, E. C., Lee, K. M. & Wong, K. B. Structures of eukaryotic ribosomal stalk proteins and its complex with trichosanthin, and their implications in recruiting ribosome-inactivating proteins to the ribosomes. *Toxins (Basel)* **7**, 638-647, doi:10.3390/toxins7030638 (2015).
23 Duval, M. *et al.* Escherichia coli ribosomal protein S1 unfolds structured mRNAs onto the ribosome for active translation initiation. *PLoS Biol* **11**, e1001731, doi:10.1371/journal.pbio.1001731 (2013).
24 Noeske, J. *et al.* High-resolution structure of the Escherichia coli ribosome. *Nat Struct Mol Biol* **22**, 336-341, doi:10.1038/nsmb.2994 (2015).
25 Tan, C. S. H. *et al.* Thermal proximity coaggregation for system-wide profiling of protein complex dynamics in cells. *Science* **359**, 1170-1177, doi:10.1126/science.aan0346 (2018).
26 Nonaka, G., Blankschien, M., Herman, C., Gross, C. A. & Rhodius, V. A. Regulon and promoter analysis of the E. coli heat-shock factor, sigma32, reveals a multifaceted cellular response to heat stress. *Genes Dev* **20**, 1776-1789, doi:10.1101/gad.1428206 (2006).
27 McHugh, J. P. *et al.* Global iron-dependent gene regulation in Escherichia coli. A new mechanism for iron homeostasis. *J Biol Chem* **278**, 29478-29486, doi:10.1074/jbc.M303381200 (2003).
28 Pomposiello, P. J., Koutsolioutsou, A., Carrasco, D. & Demple, B. SoxRS-regulated expression and genetic analysis of the yggX gene of Escherichia coli. *J Bacteriol* **185**, 6624-6632, doi:10.1128/jb.185.22.6624-6632.2003 (2003).
29 Molloy, M. P. *et al.* Proteomic analysis of the Escherichia coli outer membrane. *Eur J Biochem* **267**, 2871-2881, doi:10.1046/j.1432-1327.2000.01296.x (2000).
30 Juncker, A. S. *et al.* Prediction of lipoprotein signal peptides in Gram-negative bacteria. *Protein Sci* **12**, 1652-1662, doi:10.1110/ps.0303703 (2003).
31 Tachikawa, T. & Kato, J. Suppression of the temperature-sensitive mutation of the bamD gene required for the assembly of outer membrane proteins by multicopy of the yiaD gene in Escherichia coli. *Biosci Biotechnol Biochem* **75**, 162-164, doi:10.1271/bbb.100612 (2011).
32 Kannan, G. *et al.* Rapid acid treatment of Escherichia coli: transcriptomic response and recovery. *BMC Microbiol* **8**, 37, doi:10.1186/1471-2180-8-37 (2008).
33 Liu, Y., Bauer, S. C. & Imlay, J. A. The YaaA protein of the Escherichia coli OxyR regulon lessens hydrogen peroxide toxicity by diminishing the amount of intracellular unincorporated iron. *J Bacteriol* **193**, 2186-2196, doi:10.1128/JB.00001-11 (2011).
34 Byrne, R. T., Chen, S. H., Wood, E. A., Cabot, E. L. & Cox, M. M. Escherichia coli genes and pathways involved in surviving extreme exposure to ionizing radiation. *J Bacteriol* **196**, 3534-3545, doi:10.1128/JB.01589-14 (2014).
35 Lee, C. & Marians, K. J. Characterization of the nucleoid-associated protein YejK. *J Biol Chem* **288**, 31503-31516, doi:10.1074/jbc.M113.494237 (2013).
36 Gagarinova, A. *et al.* Systematic Genetic Screens Reveal the Dynamic Global Functional Organization of the Bacterial Translation Machinery. *Cell Rep* **17**, 904-916, doi:10.1016/j.celrep.2016.09.040 (2016).
37 Maier, L. *et al.* Extensive impact of non-antibiotic drugs on human gut bacteria. *Nature* **555**, 623-628, doi:10.1038/nature25979 (2018).
38 Nichols, R. J. *et al.* Phenotypic landscape of a bacterial cell. *Cell* **144**, 143-156, doi:10.1016/j.cell.2010.11.052 (2011).
39 Sargentini, N. J., Gularte, N. P. & Hudman, D. A. Screen for genes involved in radiation survival of Escherichia coli and construction of a reference database. *Mutat Res* **793-794**, 1-14, doi:10.1016/j.mrfmmm.2016.10.001 (2016).